

Process length variation of the cyst of the dinoflagellate *Protoceratium reticulatum* in the North Pacific and Baltic-Skagerrak region: calibration as an annual density proxy and first evidence of pseudo-cryptic speciation

JQS

KENNETH NEIL MERTENS,^{1*} MANUEL BRINGUÉ,² NICOLAS VAN NIEUWENHOVE,³ YOSHIHITO TAKANO,⁴ VERA POSPELOVA,² ANDRE ROCHON,⁵ ANNE DE VERNAL,⁶ TAOUIK RADJ,⁶ BARRIE DALE,⁷ R. TIMOTHY PATTERSON,⁸ KAARINA WECKSTRÖM,⁹ ELINOR ANDRÉN,¹⁰ STEPHEN LOUWYE¹ and KAZUMI MATSUOKA¹¹

¹Research Unit Palaeontology, Ghent University, Krijgslaan 281 S8, 9000 Gent, Belgium

²School of Earth and Ocean Sciences, University of Victoria, BC, Canada

³GEOTOP, Université du Québec à Montréal, Québec, Canada and GEOMAR, Helmholtz Centre for Ocean Research Kiel, Germany

⁴Institute for East China Sea Research (ECSER), Nagasaki, Japan

⁵Institut des sciences de la mer de Rimouski (ISMER), Université du Québec à Rimouski 310, QC, Canada

⁶GEOTOP, Université du Québec à Montréal, Québec, Canada

⁷Department of Geosciences, University of Oslo, Norway

⁸Ottawa-Carleton Geoscience Centre and Department of Earth Sciences, Carleton University, Ottawa, ON, Canada

⁹Geological Survey of Denmark and Greenland (GEUS), Department of Marine Geology and Glaciology, Denmark

¹⁰School of Life Sciences, Södertörn University, Huddinge, Sweden

¹¹Institute for East China Sea Research (ECSER), Nagasaki, Japan

Received 21 March 2012; Revised 20 May 2012; Accepted 28 May 2012

ABSTRACT: Process length variation of cysts of the dinoflagellate *Protoceratium reticulatum* (Claparède et Lachmann) Bütschli in surface sediments from the North Pacific was investigated. The average process length showed a significant inverse relation to annual seawater density: $\sigma_{\text{T annual}} = -0.8674 \times \text{average process length} + 1029.3$ ($R^2 = 0.84$), with a standard error of 0.78 kg m^{-3} . A sediment trap study from Effingham Inlet in British Columbia revealed the same relationship between average process length and local seawater density variations. In the Baltic–Skagerrak region, the average process length variation was related significantly to annual seawater density: $\sigma_{\text{T annual}} = 3.5457 \times \text{average process length} - 993.28$ ($R^2 = 0.86$), with a standard error of 3.09 kg m^{-3} . These calibrations cannot be reconciled, which accentuates the regional character of the calibrations. This can be related to variations in molecular data (small subunit, long subunit and internal transcribed spacer sequences), which show the presence of several genotypes and the occurrence of pseudo-cryptic speciation within this species. Copyright © 2012 John Wiley & Sons, Ltd.

KEYWORDS: Baltic-Skagerrak; Effingham Inlet; sediment trap; SSS; SST.

Introduction

The reconstruction of ocean salinity is crucial in our understanding of past oceanic circulation and paleoclimate (e.g. Hay, 2008) because together with temperature it determines density, which steers changes in the thermohaline circulation (e.g. Rahmstorf, 2002). Salinity has been estimated using different methods, for instance coupled Mg/Ca – $\delta^{18}\text{O}$ measurements on foraminifera (e.g. Schmidt and Spero, 2011) and δD in alkenones (e.g. van der Meer *et al.*, 2008). However, most of these approaches suffer from large uncertainties in the reconstructed values (e.g. Rohling, 2000). The search for an unequivocal approach demands further investigation into reliable paleosalinity proxies. Research on the potential of process length variation of dinoflagellate cysts as a salinity proxy was initiated by observations by Wall *et al.* (1973) on Black Sea dinoflagellate cysts, in particular those produced by *Lingulodinium polyedrum* (Stein) Dodge. First attempts to quantify salinity through morphological measurements relied on culture studies (e.g. Hallett, 1999). Subsequent studies on cysts of *Lingulodinium polyedrum* and *Protoceratium reticulatum* (Claparède et Lachmann) Bütschli extracted

from surface sediments (Mertens *et al.*, 2009, 2010) revealed a significant relationship between process length and salinity. The latter study also revealed a potential additional influence of temperature on process length, highlighting the possible importance of seawater density on this feature. Because of its cosmopolitan occurrence (Wall *et al.*, 1977) and its biostratigraphical range down to the mid-Pliocene (De Schepper *et al.*, 2009), morphological variations of the cysts of *P. reticulatum* have the most potential in paleoreconstruction. Therefore, this study investigates process length variation of cysts of *P. reticulatum* in the North Pacific and its relationship to salinity and temperature. We show that process length variation correlates with density, and its potential application as a regional density proxy is investigated. Furthermore, this study shows that these measurements cannot be reconciled with a combination of new and previously published measurements from the Baltic–Skagerrak system (Mertens *et al.*, 2010). In addition, we show that this discrepancy can be related to genetic differences: molecular data [small subunit (SSU), large subunit (LSU) and internal transcribed spacer (ITS) rRNA gene sequences] revealed consistent differences between ITS sequences from the Kattegat (Sweden), British Columbia (Canada) and Lake Saroma (Japan), suggesting the occurrence of pseudo-cryptic speciation.

*Correspondence: K. N. Mertens, as above.

E-mail: kenneth.mertens@ugent.be

Oceanographic context

The oceanography of the North Pacific can be described using the largest active current systems (Fig. 1). In the western North Pacific two major currents are present around Japan, namely the cold Oyashio Current and the warm Kuroshio Current, from which the warm Tsushima Current branches. The warm Kuroshio Current originates in the Philippines, flows along the east coast of Taiwan into the southern part of the East China Sea, and then branches to form the Tsushima Current. The main

part of the Kuroshio Current flows along the southern coast of West Japan, sometimes forming a large gyre. The physico-chemical character of the Kuroshio Current changes from south to north but it is generally characterized by low nutrient levels, lower density and high temperatures (e.g. Teramoto, 1987). The Oyashio (or Kuril) Current flows southward from the north-western Pacific and the Bering Sea along the east coast of Hokkaido. This current is characterized by low temperature, higher density and high biogenic productivity induced by high nutrient contents (e.g. Kusakabe *et al.*, 2002). East of Japan, the

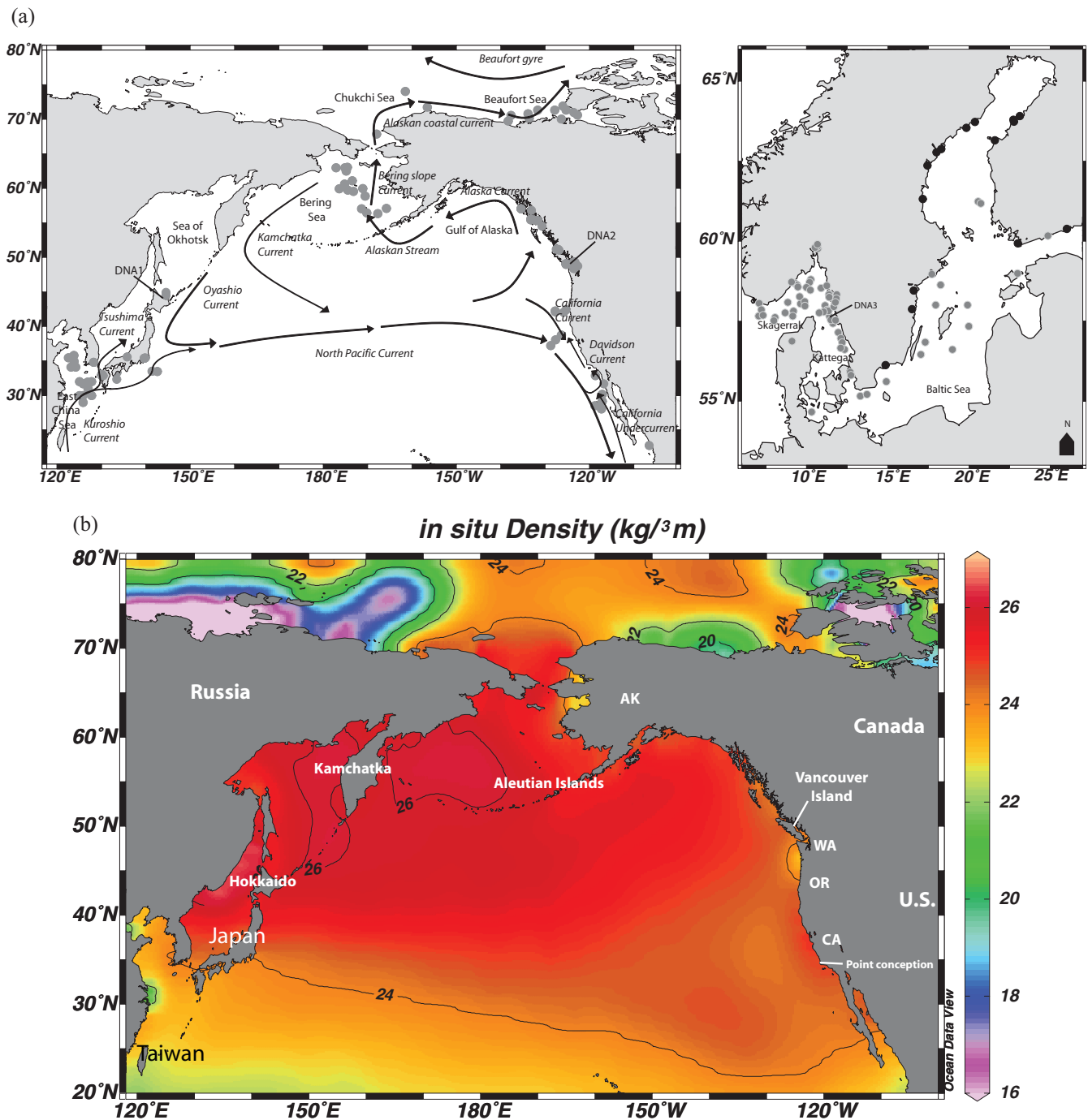


Figure 1. (a) Left: distribution of the studied surface samples in the North Pacific (grey circles). The largest active current systems in the North Pacific are indicated by arrows (current names are in italics and discussed in the text). The sampling locations for molecular analysis are also shown (DNA1, Saroma Lake, Japan; DNA2, Brentwood Bay, B.C., Canada). Right: distribution of the studied surface samples in the Baltic Sea. Samples studied by Mertens *et al.* (2010) are shown with dark grey circles, newly studied samples by black circles. Locations of Skagerrak, Kattegat and Baltic Sea are indicated. The sampling location for molecular analysis in the Swedish coast of the Kattegat is also shown (DNA3). (b) Density variations in the North Pacific as derived from the World Ocean Database 2001 with indication of geographic locations mentioned in the text: Canada, Japan, Russia, Taiwan and United States (U.S.) (AK, Alaska; CA, California; OR, Oregon; WA, Washington).

warm Kuroshio Current and cold Oyashio Current meet to form the North Pacific Current.

In the eastern North Pacific, the North Pacific Current splits into the southward California Current and the northward Alaska Current. The California Current System consists of the California Current, the Davidson Current and the California Undercurrent (Hickey, 1998). The California Current carries relatively cold, nutrient- and oxygen-rich subarctic waters southward along the Pacific coast of the United States from the Washington–Oregon border to southern California. South of Point Conception, a segment of the California Current turns south-eastward, then shoreward and northward to become the Southern California Countercurrent. The California Undercurrent is a narrow current that originates in the eastern equatorial Pacific and transports warmer, saline, phosphate-rich, oxygen-poor water northward over the continental slope. The Davidson Current is a seasonal surface current that flows northward over the shelf zone from Point Conception to Vancouver Island during autumn and winter. The regional oceanography of the estuarine environment of British Columbia is described in detail by Radi *et al.* (2007).

To the north, the easterly flow of the North Pacific Current together with the northward-flowing Alaska Current results in the anticlockwise circulation in the Gulf of Alaska, carrying warm Pacific waters along the southern Aleutian Islands. The Alaska Current flows into the Alaskan Stream and this current enters the cold and dense Bering Sea through the many passes in the Aleutian Arc. The circulation in the Bering Sea basin is often described as an anticlockwise gyre, with the southward-flowing cold-water Kamchatka Current forming the western boundary current along the Siberian Pacific coast and the northward-flowing Bering Slope Current forming the eastern boundary current (Stabeno *et al.*, 1999). The Kamchatka Current branches to become the Oyashio Current and to join the warmer North Pacific Current. Circulation on the eastern Bering Sea shelf is generally north-westward, into the Chukchi Sea, continuing to the Beaufort Sea via the Alaskan coastal current. The hydrography of the Bering and Chukchi seas is further detailed by Radi *et al.* (2001). All along the Beaufort Sea coast the currents are influenced by wind direction, which alternates between eastward in the Canadian Archipelago and westward beyond the Mackenzie Trough (Vilks *et al.*, 1979). Offshore, the clockwise Beaufort Gyre dominates the mean, large-scale movement of sea ice and surface water (Coachman and Aagaard, 1974).

Material and methods

Surface sediment study: sample preparation and light microscopy

Biometric measurements utilizing cysts of *P. reticulatum* were carried out on specimens recovered from 137 surface sediment samples from the North Pacific (Fig. 1). The dinoflagellate cyst assemblages were previously studied for 86 of the 137 samples (Matsuoka, 1981; Matsuoka *et al.*, 2003; Cho and Matsuoka, 2001; Radi *et al.*, 2001, 2007; Pospelova *et al.*, 2008; Richerol *et al.*, 2008; Krepakevich and Pospelova, 2010; Limoges *et al.*, 2010; Pospelova and Kim, 2010). Specimens from an additional 15 samples obtained from the Baltic Sea (Fig. 1a) were also examined to obtain more modern analogues from a low-salinity environment, complementing previously published data (Mertens *et al.*, 2010).

Most samples were core top samples obtained from areas with relatively high sedimentation rates and can be considered recent, i.e. representing tens of years to a few centuries. It is assumed here that the environmental conditions affecting the

morphological changes within the cysts are relatively similar to recent environmental conditions.

All the cysts were extracted from the sediments using methods described in the respective literature (Supporting information, Table S1). Most were standard palynological methods involving hydrochloric acid and hydrofluoric acid, sieving and/or sonication. Aliquots of residue were mounted in glycerine gelatine jelly. Regardless of the extraction method, comparison of cysts processed using different methodologies showed no preservational biasing (Fig. 2). This suggests that different processing methods had no effect on measurements, as previously observed by Mertens *et al.* (2009). However, slides from samples that were processed using an additional step involving the addition of 1% potassium hydroxide (KOH) treatment heated to 70°C in a warm water bath (Matsuoka *et al.*, 1989) were discarded and reprocessed as KOH treatment causes swelling of cysts (Mertens *et al.*, 2009).

All measurements and light photomicrographs were obtained by K.N.M., M.B. and N.V.N., respectively, using an Olympus BX51 with a Nikon digital sight DS-1L 1 module, a Nikon eclipse 80i microscope and coupled Nikon DS Camera Head (DS-Fi1)/DS Camera Control Unit DS-L2 and a Leica DM 5000 B equipped with a Leica DFC490 camera and Leica Application Suite 2.8.1 software, all with 100× oil-immersion objectives. For each sample, the length of the three longest visible processes on one cyst and its largest body diameter were measured for 50 cysts per sample, when possible. Measuring 50 cysts yields reproducible results (Mertens *et al.*, 2010) with the average process length per sample for cysts of *P. reticulatum* being reliably reproduced between the observers, within $\pm 0.5 \mu\text{m}$. The length of each process was measured from the middle of the process base to the process tip. To reduce the chance of observer bias only specimens carrying processes with characteristic platforms and hooklets were measured for morphological analysis. For the same reason no cysts lacking processes (i.e. 'zero' process length) were included in the analysis, due to the difficulty in confidently identifying such specimens. Such specimens were rarely encountered in a few samples collected from the Baltic Sea. For each cyst, three processes could always be found with the focal plane of the light microscope at the optical section of the central cyst body, and thus this number seemed a reasonable option. Three reasons can be advanced for choosing measurement of the longest processes: (i) the longest processes reflect unobstructed cyst growth; (ii) measuring the longest processes increases the accuracy of the proxy as it documents the largest variation; and (iii) because only a few processes were parallel to the focal plane of the microscope, it was imperative to make a consistent choice. Sometimes fewer than 50 cysts were measured, if more were not available. Fragments representing less than half of a cyst were not measured, nor were cysts with mostly broken processes.

Summer and annual sea surface temperature (SST), sea surface salinity (SSS), the ratio between salinity and temperature (SSS/SST) and seawater density (σ_t) at different depths were interpolated using the gridded 0.25° World Ocean Atlas (WOA) 2001 (Conkright *et al.*, 2002) and the Ocean Data View software (Schlitzer, 2010). The WOA 2001 is generated from the World Ocean Database 2001, which covers 7.9 million data points of historical and modern oceanographic data. Here the WOA 2001 is used as it has a 0.25° resolution compared with the lower 1° resolution WOA 2005, which was used in Mertens *et al.* (2009). Biometric measurements on cysts from the different study areas were compared with SST, SSS, SSS/SST and σ_t by calculating the coefficient of determination R^2 . The significance of the coefficient of determination R^2 was calculated using a *t*-test.

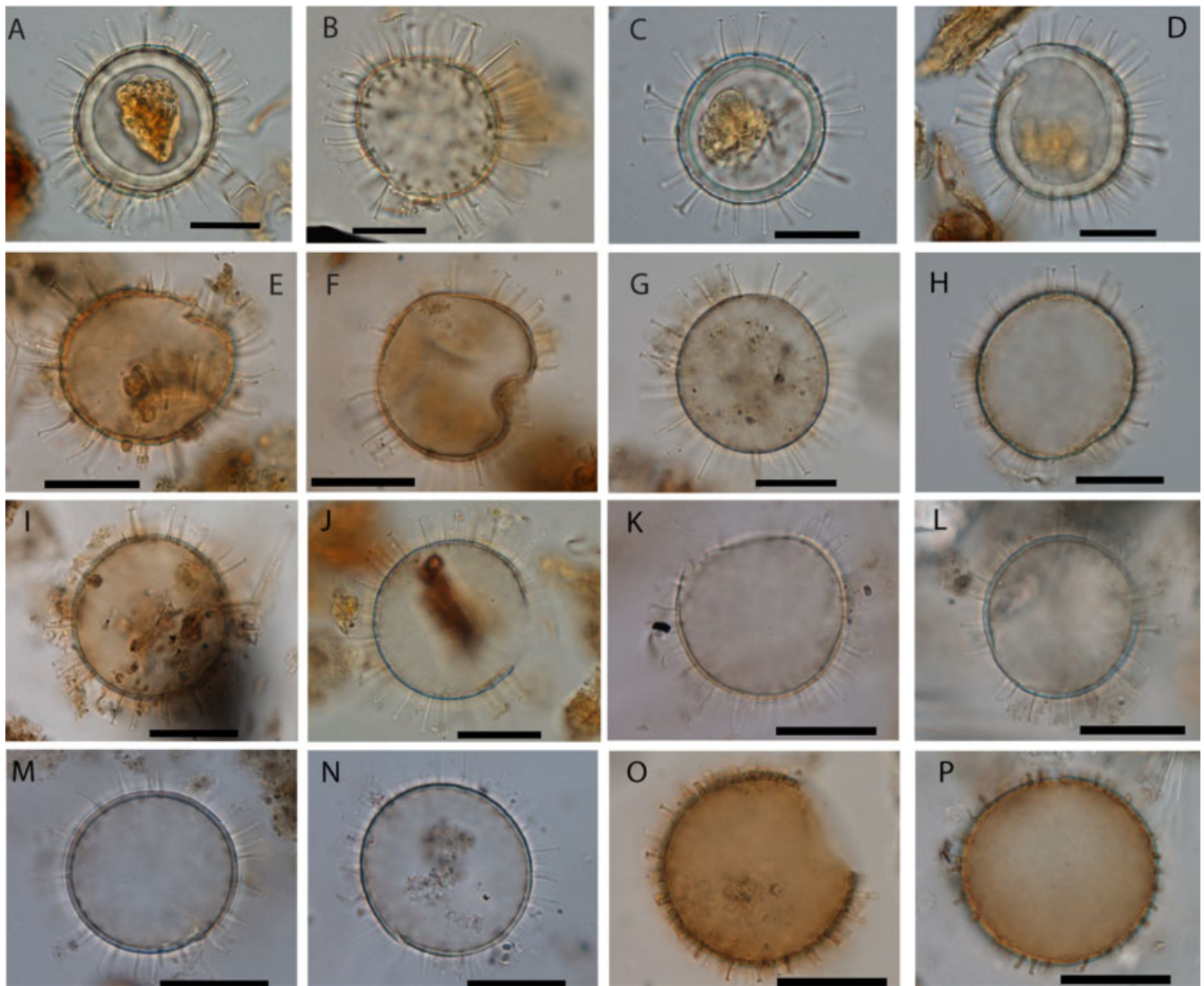


Figure 2. Morphological variation of cysts of *Protoceratium reticulatum* in the North Pacific, sorted from long (A) to reduced processes (P). A and B are from Saanich Inlet, off Boatswain Bank (07-890). (A) Large specimen with cell contents and with extremely long and often merged processes; (B) large specimen with pear-shaped body, note pronounced asymmetrical distribution of process lengths. C and D are from Strait of Georgia (cm3). Two long-process-bearing specimens with cell contents. E and F are from the Gulf of Tehuantepec (St. 3). G and H are from near Petersburg (11, 13). I is from Seymour Belize Inlet (SB1). J is from Effingham Inlet (UVic 06-312). K is from Tokyo Bay (TK22). L is from off Kochi (KT88-16Y). M and N are from East China Sea (C9, Y1). O is from Bering sea (TT51-295). P is from Chukchi sea (SI689-22). Scale bars = 20 μm . This figure is available in colour online at wileyonlinelibrary.com/journal/jqs.

Sediment trap study and downcore study from Effingham Inlet, British Columbia

Identical morphological measurements were also applied to 33 sediment trap samples from Effingham Inlet by Kenneth N. Mertens (Fig. 3; supporting Table S2). Effingham Inlet dinoflagellate cysts were previously studied by Kumar and Patterson (2002) and Patterson *et al.* (2005). The number of specimens with cell contents was also noted.

A mooring equipped with an Oregon State University (OSU) Tracer 15 sequencing sediment trap was deployed inside the inner basin (49°04.319'N, 125°09.475'W) in May 1999 at ~30 m above the bottom (Fig. 3). This trap has a collection area of 0.49 m² and consists of 14 sequential sample collection cylinders timed to rotate every 8–15 days, depending on the anticipated length of mooring deployment. Cylinder solutions were composed of filter seawater (GFF and/or 0.2 μm Nucleopore), supplemented with 4 g L⁻¹ sodium azide to prevent bacterial decomposition yet minimize solubilization of metals, and 3 g L⁻¹ sodium chloride to prevent mixing between

ambient and cylinder seawater. The mooring and the trap were replaced approximately every 6 months, for a total deployment of 16 months (490 days).

Trap materials from 33 cylinders, encompassing the period between 29 May 1999 and 13 July 2000, were analysed. Trap materials were collected from the cylinders at the end of each collection interval and divided into six subsamples using an air-driven precision plankton splitter. Salts from the trap solutions were removed with pH-adjusted (8.0) deionized water. The samples were subsequently dried in a desiccator. These samples were also processed using a standard palynological processing technique (Pospelova *et al.*, 2004).

Molecular analysis

Surface samples were collected from Brentwood Bay (48.57°N, 123.47°W, 5 m water depth) in Saanich Inlet, British Columbia, Canada (sampled on 1 October 2011, with a Petite Ponar Grab), station 2 (44.12°N, 143.87°E, 18.3 m water depth) from Lake Saroma, Hokkaido, Japan (TFO core sample, sampled on

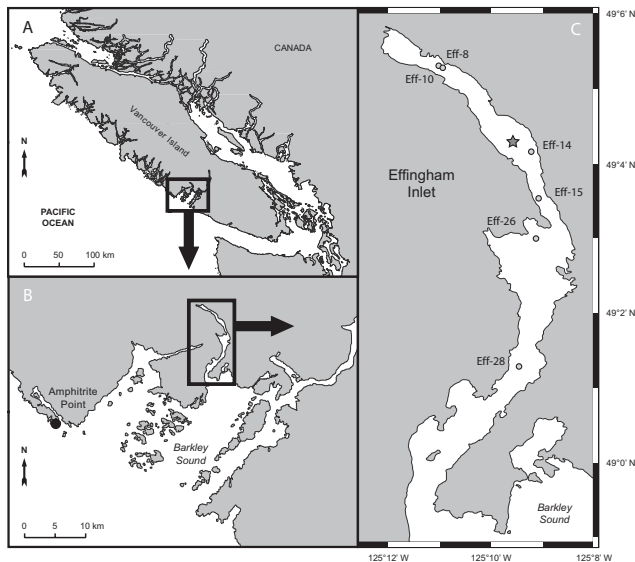


Figure 3. (A) Location of Effingham Inlet within Vancouver Island (British Columbia, Canada); (B) location of Amphitrite Point (where environmental parameters were measured) and Effingham Inlet within Barkley Sound; (C) location of Effingham Inlet inner basin sediment trap (star) and surface samples studied (filled circles).

22 July 2011) (Fig. 1a) and station Gote3 (57.50°N, 11.80°E, 28 m water depth) at the Swedish coast of the Kattegat (boxcore sampled in May 2010) (Fig. 1a). Cysts were isolated from the sediment using heavy liquid separation as described by Bolch (1997). We used cysts from the Kattegat and Lake Saroma and germinated cells from Brentwood Bay for molecular analyses. Isolated cysts were sonicated in a 200- μ L PCR tube with sterilized seawater. The cysts and the cells were individually transferred to a glass slide covered with a frame of vinyl tape, and photographed using an Olympus BX51 microscope with an Olympus DP71 digital camera. The cell was transferred to an inverted microscope and crushed with a fine glass needle, and subsequently transferred into a 200- μ L PCR tube containing 3 μ L Milli-Q water. We determined sequences of ITS regions (internal transcribed spacer 1–5.8 rRNA – ITS2) and partial sequences of SSU and LSU rRNA from single cysts and cultured cells. In the first round of PCR, the external primers (SR1 and LSU R2; Takano and Horiguchi, 2005) were used with PCR

mixtures of KOD-Plus-Ver. 2 Kit (Toyobo, Osaka, Japan) and the PCR conditions were: one initial cycle of denaturation at 94 °C for 2 min, followed by 35 cycles of denaturation at 94 °C for 30 s, annealing at 50 °C for 30 s, and extension at 72 °C for 2 min and final extension at 72 °C for 5 min. In the second round of PCR, two sets of primers (SR12cF and 25R1, LSU D1R and LSU R2; Takano and Horiguchi, 2005) were used with PCR mixtures of KOD-Plus-Ver. 2 Kit (Toyobo), 0.5 μ L of the first-round PCR product as DNA template, and the same PCR conditions except for extension at 72 °C for 1 min. In the third round of PCR, three sets of primers (SR12cF and 25F1R, LSU D1R and 25R1, LSU D3A and LSU R2; Takano and Horiguchi, 2005) were used with PCR mixtures of the TaKaRa EX taq system (Takara Bio Inc., Shiga, Japan), 0.5 μ L of the second-round PCR products as DNA template, and the same PCR conditions except for extension at 72 °C for 30 s. PCR products were sequenced directly using the ABI PRISM BigDye Terminator Cycle Sequencing Kit (Perkin-Elmer, Foster City, CA, USA). We sequenced both the forward and the reverse strands. The sequences obtained were manually aligned. These techniques are modifications of the methods described by Takano and Horiguchi (2005).

Results

Process length variation in surface sediments

Overall cyst biometrics

For the 137 samples from the North Pacific, the 15 051 process length measurements averaged 7.15 μ m (ranging from 0.5 to 17.6 μ m) with a standard deviation of 2.46 μ m (Fig. 4A). Several morphotypes have been described for the cyst of *P. reticulatum* (= *Operculodinium centrocarpum sensu* Wall and Dale, 1966), based on variations in process length: *O. centrocarpum* Arctic morphotype of de Vernal *et al.* (2001) (=type B of de Vernal *et al.*, 1989) and *O. centrocarpum* var. *cezare* of de Vernal *et al.* (1989). It is particularly notable that some of the short-process-bearing specimens occurring in the Baltic Sea (Mertens *et al.*, 2010) are indistinguishable from *O. centrocarpum* form B of de Vernal *et al.* (1989), here encountered in the Bering and Chukchi seas (Radi *et al.*, 2001) and the Beaufort Sea (Richerol *et al.*, 2008). The 2561 body diameter measurements utilized gave an average body diameter of 37.6 μ m with a standard deviation of 4.4 μ m, over a

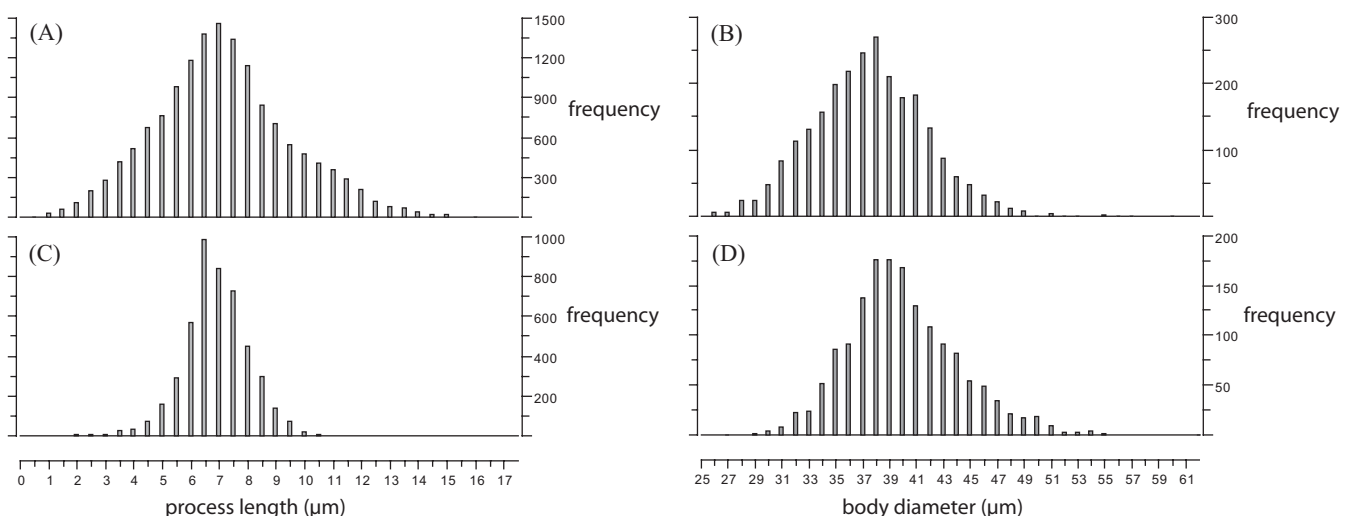


Figure 4. Size–frequency curves. (A) Size–frequency curve of the 15 051 process length measurements in the surface sediments from the North Pacific. (B) Size–frequency curve of the 2561 body diameter measurements in the surface sediments from the North Pacific. (C) Size–frequency curve of the 4842 process length measurements from the sediment trap samples from Effingham Inlet. (D) Size–frequency curve of the 1641 body diameter measurements from the sediment trap samples from Effingham Inlet.

Table 1. Coefficient of determination R^2 calculated between environmental parameters and average process length of cysts of *Protoceratium reticulatum*.

	Process length (Baltic– Skagerrak)	Process length (North Pacific)	Process length (Baltic– Skagerrak + North Pacific)
Annual SST	+0.81*	+0.08	+0.12
Annual SSS	+0.87*	+0.64	+0.30
Annual SSS/SST	+0.84*	+0.00	+0.00
Annual σ_t	+0.86*	+0.84*	+0.29
Summer SST	+0.48	+0.01	+0.01
Summer SSS	+0.86*	+0.65	+0.27
Summer SSS/SST	+0.85*	+0.13	+0.02
Summer σ_t	+0.86*	+0.72	+0.26
Autumn SST	+0.75*	+0.08	+0.14
Autumn SSS	+0.88*	+0.07	+0.42
Autumn SSS/SST	+0.85*	+0.00	+0.00
Autumn σ_t	+0.87*	+0.25	+0.41
Winter SST	+0.70	+0.16	+0.21
Winter SSS	+0.87*	+0.58	+0.34
Winter SSS/SST	+0.05	+0.03	+0.01
Winter σ_t	+0.87*	+0.81*	+0.34
Spring SST	+0.81*	+0.18	+0.25
Spring SSS	+0.85*	+0.66	+0.24
Spring SSS/SST	+0.71	+0.03	+0.01
Spring σ_t	+0.85*	+0.84*	+0.22

* Significant correlations using the t -test ($P < 1 \times 10^{-25}$). SST, sea surface temperature; SSS, sea surface salinity; σ_t , seawater density.

range from 25.5 to 59.5 μm (Fig. 4a). The 15 extra samples obtained from the Baltic Sea show very similar spectra to samples studied by Mertens *et al.* (2010). Reduced specimens in the Baltic Sea with shorter processes resemble *O. centrocarpum* var. *cezare* of de Vernal *et al.* (1989). However, that morphology is not recorded in the North Pacific.

Correlations between the morphological measurements and environmental parameters using a reduced dataset

All samples containing fewer than 20 measured cysts were excluded from the analysis, in this case 37 of the 137 samples obtained from the North Pacific. Seven samples from the Beaufort Sea were deemed outliers based on the lack of reliable interpolations from the World Ocean Atlas 2001; these points were also excluded from the calibration. An extra eight samples from the deep California margin (water depths >2000 m) were excluded as outliers as they were probably transported (cf. *infra*). These restrictions resulted in a reduced dataset of 85 out of 137 samples from the North Pacific.

The coefficient of determination R^2 was calculated between average process length and SSS, SST, SSS/SST and σ_t at different water depths, both annually and seasonally for the samples from the North Pacific, the Baltic–Skagerrak area and for the combined dataset (Table 1). For the 85 samples from the North Pacific, the most significant linear correlation was with annual water density ($R^2 = 0.84$; $P < 1 \times 10^{-25}$). Significant linear correlations were also found with spring water density ($R^2 = 0.84$) and winter water density ($R^2 = 0.81$), but none for any of the other parameters. For the 83 Baltic–Skagerrak samples – 15 new samples complementing the previously published 68 samples from the Baltic–Skagerrak system from Mertens *et al.* (2010) – significant correlations were found for nearly all parameters studied ($P < 1 \times 10^{-25}$) (Table 1). This was related to the covariation of salinity with temperature in

Table 2. The coefficient of determination calculated between environmental parameters and average body diameter of cysts of *Protoceratium reticulatum*

	Body diameter (Baltic– Skagerrak)	Body diameter (North Pacific)	Body diameter (Baltic– Skagerrak + North Pacific)
Annual SST	+0.38	+0.05	+0.01
Annual SSS	+0.38	+0.70	+0.02
Annual SSS/SST	+0.36	+0.00	+0.00
Annual σ_t	+0.38	+0.49	+0.03
Summer SST	+0.32	+0.13	+0.06
Summer SSS	+0.38	+0.65	+0.02
Summer SSS/SST	+0.36	+0.00	+0.01
Summer σ_t	+0.37	+0.30	+0.03
Autumn SST	+0.34	+0.04	+0.01
Autumn SSS	+0.39	+0.17	+0.07
Autumn SSS/SST	+0.38	+0.00	+0.00
Autumn σ_t	+0.39	+0.02	+0.08
Winter SST	+0.23	+0.01	+0.00
Winter SSS	+0.38	+0.72	+0.04
Winter SSS/SST	+0.10	+0.01	+0.01
Winter σ_t	+0.38	+0.60	+0.04
Spring SST	+0.40	+0.00	+0.01
Spring SSS	+0.37	+0.71	+0.01
Spring SSS/SST	+0.27	+0.01	+0.00
Spring σ_t	+0.37	+0.57	+0.01

There were no significant correlations using the t -test ($P < 1 \times 10^{-25}$). SST, sea surface temperature; SSS, sea surface salinity; σ_t , seawater density.

the Baltic–Kattegat–Skagerrak estuarine system. The correlation of average process length to SSS and σ_t was larger than to SST or SSS/SST, both on an annual and a seasonal scale. When using the dataset containing all 168 samples from both the Baltic–Skagerrak area and the North Pacific, no significant correlations were found with any of the parameters studied (Table 1).

Similar coefficients of determination R^2 were also calculated for body diameter (Table 2). For the 85 samples from the North Pacific, the highest linear correlations were with SSS ($R^2 = \sim 0.7$), but these were not significant at $P < 1 \times 10^{-25}$. Also, for the 83 Baltic–Skagerrak samples, no significant correlations were found for all parameters studied (Table 2). For the 168 samples from both the Baltic–Skagerrak and the North Pacific, no significant correlations were found with any of the parameters studied (Table 2).

No significant correlation was found between the process length and cyst body diameter in the Baltic Sea ($R^2 = 0.35$) and in the North Pacific ($R^2 = 0.51$).

In the Baltic Sea and North Pacific, no significant correlation was found between relative abundances of cysts of *P. reticulatum* and average process length ($R^2 = 0.45$ and 0.02, respectively), nor body diameter ($R^2 = 0.34$ and 0.06, respectively).

Process length variation in Effingham Inlet sediment trap

Overall cyst biometrics

For the 33 samples from the Effingham Inlet sediment trap, the 4842 process length measurements averaged 6.87 μm with a standard deviation of 1.23 μm , and ranged from 1.8 to 13.1 μm (Fig. 4C). Average process lengths of surface sediment samples in the immediate vicinity of the trap (EFF-14, EFF-15, EFF-26) (Fig. 3) were very similar (between 6.74 and 6.94 μm). The

1614 body diameter measurements gave an average body diameter of $40.1\ \mu\text{m}$ with a standard deviation of $4.3\ \mu\text{m}$, over a range from 26.8 to $61.5\ \mu\text{m}$ (Fig. 4D).

Correlations between the environmental parameters and average process length variation

Maximum SST recorded at the Amphitrite Point on southwestern Vancouver Island (Fig. 2) occurred from mid-July to mid-September, with an average of 12.5°C in 1999 and 13.2°C in 2000 (Fig. 5). Minimum SST occurred from January to March with an average of 7.9°C . Marked changes in SSS can be observed at the Amphitrite Point during October 1999 to April 2000 because of intensified precipitation (Fig. 5). A minimum

of 25.5 psu (practical salinity unit) was recorded in November 1999, and a maximum of 33.5 psu during June 2000. The fluctuations of seawater density covary strongly with SSS fluctuations.

When SST, SSS and density records from the Amphitrite Point are visually compared with the recorded average process length variation (Fig. 5) very similar fluctuations between the reversed average process length and both SSS and density are observed with no obvious similarities to the SST record. It is also notable that a greater number of cysts with cell contents were found during summer 1999 (Fig. 5). However, correlation coefficients between observed parameters and process length are not significant ($R^2 < 0.10$). Furthermore, given a measurement error of $\pm 0.5\ \mu\text{m}$, a maximum process length of $7.27\ \mu\text{m}$ and

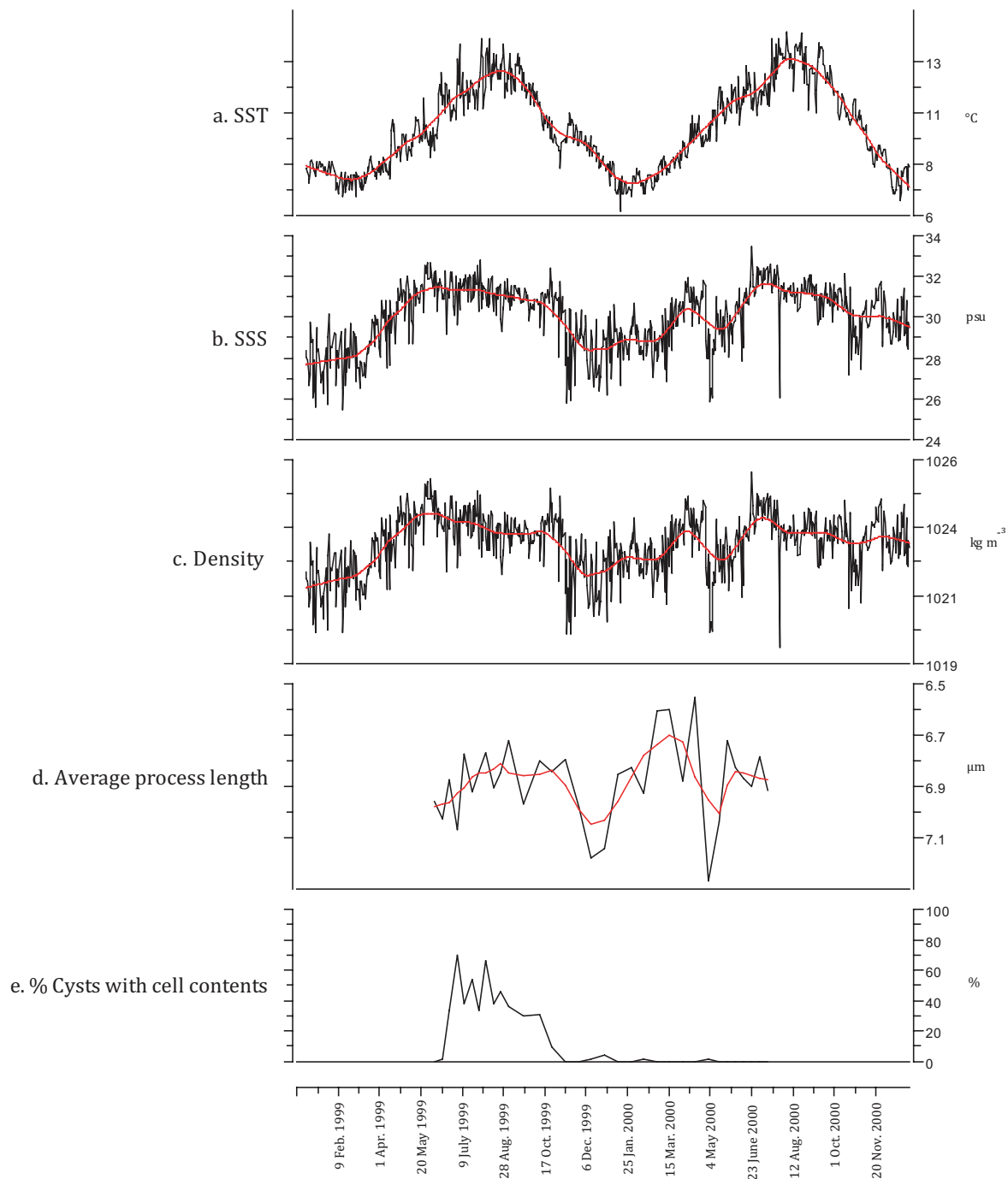


Figure 5. SST (a), SSS (b) and seawater density (c) as measured at Amphitrite Point, between 1 January 1999 and 31 December 2000. Average process length variation (note reversed scale) (d) and percentage cysts with cell contents (e) between 29 May 1999 and 13 July 2000 as recorded in the Effingham Inlet sediment trap. This figure is available in colour online at wileyonlinelibrary.com/journal/jqs.

minimum process length of 6.55 μm , the fluctuations are not statistically significant.

Molecular analysis

We determined sequences of SSU (1730 bp), ITS regions (535 bp) and partial LSU rRNA (1324 bp) genes from two single cysts from Saroma Lake, Hokkaido, Japan (AB727654), four single cysts from the Swedish coast of the Kattegat (AB727655) and one strain established from a cyst from Brentwood Bay, British Columbia, Canada (AB727656). One of the sequenced cysts from each locality is shown in Fig. 6. Comparisons of the obtained LSU and SSU sequences from the three localities show that they are identical. However, we did find significant and consistent differences in the ITS sequences, in the regions between 3 and 6 bp, and show that each of the three locations possesses a different genotype. Additionally, the Victoria sample had one degenerate site: Y=T and C. At the same site, Kattegat and Saroma had a T.

Discussion

The results from the surface sediment calibration suggest a significant correlation between average process length and seawater density. Although in the North Pacific a relatively high correlation between body diameter and salinity was found (Table 2), no significant relations were found for the other parameters and other regions. Therefore, the size variation of the cysts is suggested to be an artifact as cysts sometimes become compressed or torn, resulting in an anomalously large body diameter (see also Mertens *et al.*, 2010), or to be controlled by other environmental parameters such as regional productivity. This, together with the non-significant correlation between body diameter and process length, suggests that body diameter cannot be used to increase the accuracy of our proxy.

Factors affecting the reliability of average process length as a density proxy

Timing of cyst production

There have been very few studies on cyst production of *P. reticulatum* carried out in the North Pacific. In sediment trap studies, the cyst is often recorded throughout the year, showing one or more peaks in production. In the Strait of Georgia this species is present year-round, and showed a peak of cyst production in August 1997 (Pospelova *et al.*, 2010). Price and Pospelova (2011) record the year-round presence of this

species in a sediment trap from Saanich Inlet, with high numbers present even during the winter months. The sediment trap study from Effingham Inlet also records a year-round production of cysts, with a peak during early summer, as evidenced by a high number of cysts with cell content (Fig. 5). The monospecific 'blebs' of cysts of *P. reticulatum* within sublaminae of thin sections of Effingham Inlet sediments distinguished by Chang *et al.* (2003) could correspond to such enhanced summer production. Fujii and Matsuoka (2005) occasionally recorded this species in a sediment trap from Omura Bay, south-west Japan. In a plankton study from Okkirai Bay in northern Japan, the motile stage is recorded throughout the year, and peaks through the summer (Koike *et al.*, 2006). This last study also shows a vertical distribution of motile cells in the water column, and suggests dominant sea surface production of motile cells. We therefore assume that cyst production occurs predominantly in surface waters. The year-round production of cysts together with surface presence of motile stages thus suggests that process length will reflect annual environmental conditions at the sea surface. More sediment trap studies could shed further light on this issue. It is possible that resuspension during storm events disturbs the sediment trap signals. However, very high productivity of dinoflagellate cysts in all these studies suggests that such disturbances would be minor.

Transport issues

It could be suggested that the linear regression shown in Fig. 6 is spurious because of non-homogeneity in the dataset. Indeed, the morphological clusters in Fig. 7 individually do not show a significant linear relation to density within the individual sample areas. There is no reason, however, to assume that the proposed relationship between process length and density is not causal. Process length variation of cysts formed in culture at different salinities by a closely related species, *Lingulodinium polyedrum*, shows homogeneity in the relationship to salinity (Hallett, 1999). The non-significance of the clusters is rather interpreted to be caused by lateral transport of cysts within the individual sample areas that would mix the individual density responses and cause an overrepresentation of the most widespread morphotypes, particularly in areas with low sedimentation rates. Such mixing can thus reduce the precision for reconstruction of local densities. This can be solved through studying a number of cores and averaging out for the reconstruction of a regional signal (Mertens *et al.*, 2010) and/or applying a multi-proxy approach as proposed by Mix *et al.* (2000). Individual records should be interpreted

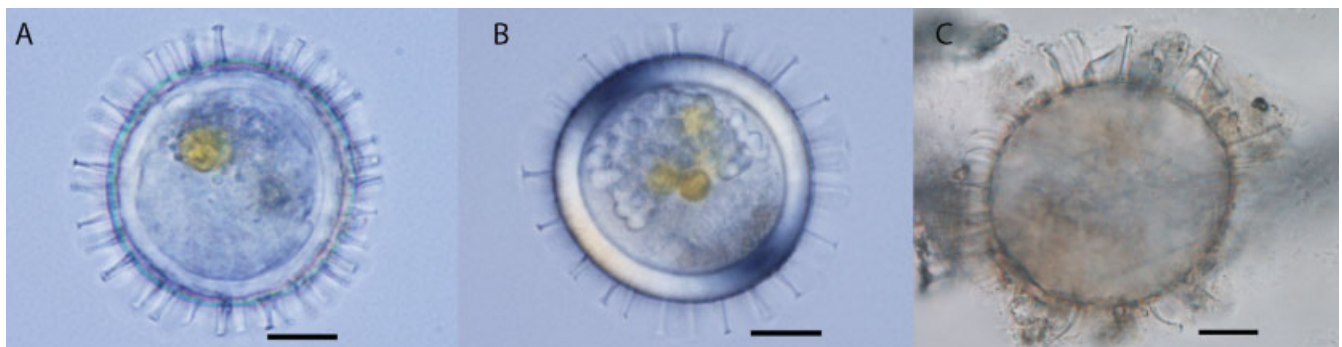


Figure 6. Examples of cysts that were sequenced from the three study areas, which had identical SSU (1730 bp) and partial LSU rRNA (1368 bp) gene sequences but small differences in ITS regions (535 bp) gene sequences. (A) Short-process-bearing cyst from Kattegat. (B) Longer-process-bearing cyst from Lake Saroma, Japan. (C) Very-long-process-bearing, large cyst that germinated from Brentwood Bay, British Columbia, the germinated cell of which was sequenced. Scale bars = 10 μm . This figure is available in colour online at wileyonlinelibrary.com/journal/jqs.

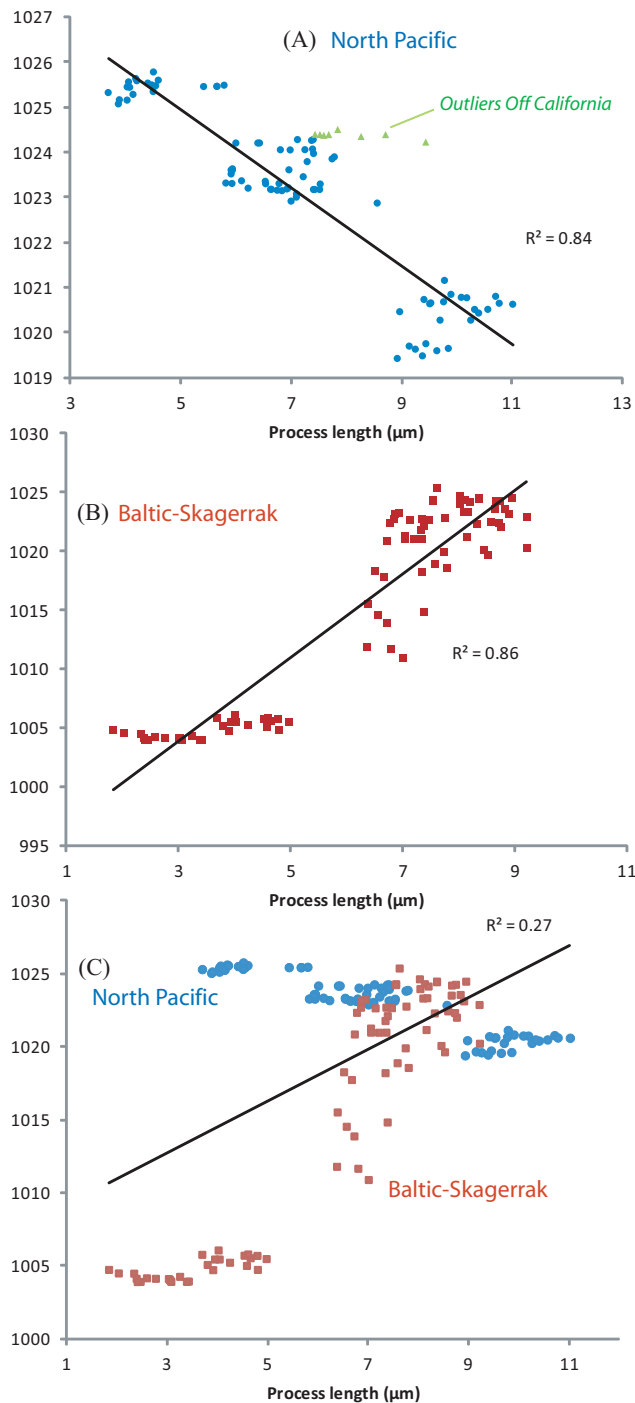


Figure 7. Relationship between average process length of cysts of *Protoceratium reticulatum* and annual density (σ_t in kg m^{-3}) and linear trendline (A) in the North Pacific (circles) showing the outliers off California that were discarded (triangles), (B) in the Baltic–Skagerrak (squares) and (C) in the North Pacific (circles) and Baltic–Skagerrak (squares). Coefficients of determination are shown. This figure is available in colour online at wileyonlinelibrary.com/journal/jqs.

with caution. We hope that further measurements from other areas can fill gaps, and/or culture experiments in this species can test for homogeneity of the relationship.

Cysts transported from the central areas of their formation can potentially influence the reliability of the environmental signal. In particular, the possibility of long-distance transport of coastal and neritic cysts into the deep sea (Dale, 1996) may limit the application of this density proxy in the open ocean. Nine of the sediment–water interface samples obtained from along the California Margin recovered from water depths

between ~2000 and ~4000 m water depth were characterized by an offset on the regression lines significant enough to warrant exclusion from being used as part of the calibration dataset (Fig. 7A). Although Pospelova *et al.* (2008) suggested a rather accurate matching of the hydrographic boundaries in this region with the changes in the cyst assemblages and concentrations, our study suggests that cysts of *P. reticulatum* are transported to these nine sites.

Construction of regional calibrations

It is notable that a particular morphotype of cysts of *P. reticulatum*, *O. centrocarpum* form B of de Vernal *et al.* (1989), occurs both in the North Pacific (Bering Sea, Chukchi Sea and Beaufort Sea) as well as in the Baltic Sea. Salinity values in the Bering Sea, Chukchi Sea and Beaufort Sea are quite different from those in the Baltic Sea: salinity varies between 26 and 33 psu (e.g. Radi *et al.*, 2001; Richerol *et al.*, 2008) in the North Pacific region and is only 5–8 psu in the Baltic Sea (e.g. Mertens *et al.*, 2010). Surface temperatures, by contrast, are quite similar: SST in the Bering Sea, Chukchi Sea and Beaufort Sea varies seasonally between the seawater freezing point (-1.9°C) and 12°C (Radi *et al.*, 2001; Richerol *et al.*, 2008), whereas the Baltic Sea temperature varies seasonally between 1 and 16°C (based on data from the World Ocean Atlas 2001). This suggests that both low density values (lower salinity values in combination with low temperatures, as exemplified in the Baltic Sea) and high density values (high salinity values in combination with low water temperatures, as exemplified in the Bering Sea, Chukchi Sea and Beaufort Sea) may lead to a reduction in process lengths and thus result in morphologically indistinguishable morphotypes.

This regional difference is obviously also reflected in regressions between process length and environmental parameters. These indicate that only annual density shows a significant linear relationship to process length both in the Baltic–Skagerrak (normal) and in the North Pacific (inverse). As in the North Pacific dataset, a similar inverse relationship to density is suggested in the sediment-trap record from Effingham Inlet, although not statistically significant (Fig. 5). This record also shows that the annual average process length is reflected in the surface sediments. Another problem is that the available environmental data were from Amphitrite Point, a site with a more open ocean setting than the sheltered Effingham Inlet (Fig. 4), which supposedly has significant differences in environmental parameters.

We therefore conclude that for the North Pacific, the following equation can be used to reconstruct annual density (σ_t) (Fig. 7A): $\sigma_{t \text{ annual}} = -0.8674 \times \text{average process length} + 1029.3$ ($R^2 = 0.84$). The standard error on the reconstructed $\sigma_{t \text{ annual}}$ value is 0.78 kg m^{-3} . For the Baltic–Skagerrak, the following equation can be utilized (Fig. 7B): $\sigma_{t \text{ annual}} = 3.5457 \times \text{average process length} - 993.28$ ($R^2 = 0.86$). The standard error for the reconstructed $\sigma_{t \text{ annual}}$ in this case is 3.09 kg m^{-3} . The North Pacific regression line connects three large clusters of process lengths: higher density morphologies (Bering Sea and Chukchi Sea), average density morphologies (Beaufort Sea, Japan and East China Sea, Effingham Inlet, Seymour Belize Inlet and similar inlets) and lower density morphologies (Saanich Inlet and Strait of Georgia). The North Pacific and Baltic–Skagerrak calibrations cannot be integrated into a single equation, as both regression lines are nearly perpendicular to each other (Fig. 7C). These results provide conclusive evidence that no linear model may be expected to explain global process length variation of cysts of *P. reticulatum* in terms of salinity, density or temperature. We therefore strongly recommend restricting application of these local

calibrations to their respective environments. It is hoped that additional measurements from other regions with very high or very low densities may eventually provide clarification. Therefore, it remains to be proven whether these calibrations from the North Pacific and the Baltic Sea can be extended to other regions. For now, average process length can be utilized as a density proxy in both regions. When corrected using an independent temperature reconstruction, salinity estimates can also be reconstructed.

*Evidence for pseudo-cryptic speciation in *P. reticulatum**

The molecular data presented here provide a first clue to why the two regions yield different relationships between process length variation and seawater density: all studied cyst morphotypes of *P. reticulatum* from Kattegat (Sweden), Lake Saroma (Japan) and Brentwood Bay (Canada) have different genotypes. These differences in the ITS sequences, together with the recorded intergradation in cyst morphology, suggest the occurrence of pseudo-cryptic speciation within this species. Such pseudo-cryptic speciation has been documented for other dinoflagellates (e.g. Montresor *et al.*, 2003; Genovesi *et al.*, 2011). Such differences also suggest that strain-specific responses are a possible factor in process length variation. This also shows that the calibration from the North Pacific contains responses from at least two different pseudo-cryptic species. This does not invalidate this proxy, however, as a mix of a number of linear responses generally results in a linear response. Other proxies tolerate this complexity: for example, the widely used alkenone-based temperature proxy is based on the production of alkenones by a large number of haptophytes, but such genetic factors seldomly disturb its application (e.g. Prah *et al.*, 2000). In our view, this merely serves to explain regional differences and stresses the need for caution and further research through the combination of molecular work combined with morphological measurements. Furthermore, it is also possible that the relationship is more complex and other factors such as the presence of sea ice, stratification (causing cyst formation in deeper water), nutrients and length of growth season or turbulence could play an accessory role in determining cyst morphology.

Conclusions

In the North Pacific, the average process length variation of cysts of *P. reticulatum* is significantly inversely related to seawater density using the following calibration: $\sigma_t \text{ annual} = -0.8674 \times \text{average process length} + 1029.3$ ($R^2 = 0.84$). These data can also be applied as a density proxy.

The average process length in specimens obtained from the Effingham Inlet sediment trap (British Columbia, Canada) is characterized by a similar inverse relationship to seawater density although it is not statistically significant. Also, this annual average process length is reflected in the surface sediments.

In the Baltic–Skagerrak region, the average process length variation of cysts of *P. reticulatum* is significantly related to seawater density with the following calibration: $\sigma_t \text{ annual} = 3.5457 \times \text{average process length} - 993.28$ ($R^2 = 0.86$).

The two calibrations can be reconciled into a single linear regression, highlighting the need to recognize their regional character.

Molecular data (SSU, ITS and LSU) sequences provide first evidence for pseudo-cryptic speciation. Further work is required to reconcile the underlying differences between both regions.

Supporting information

Additional supporting information can be found in the online version of this article:

Table S1 North Pacific and Baltic Sea surface sample details.

Table S2. Details of 33 samples from inner Basin sediment trap from Effingham Inlet.

Please note: This supporting information is supplied by the authors, and may be re-organized for online delivery, but is not copy-edited or typeset by Wiley-Blackwell. Technical support issues arising from supporting information (other than missing files) should be addressed to the authors.

Acknowledgements. Sirje Vilbaste (Estonian University of Life Sciences) is thanked for providing samples from Estonia, which unfortunately did not contain enough cysts. K.N.M. is a postdoctoral fellow of FWO Belgium, who conducted this research at the University of Victoria (British Columbia, Canada) and partly at Nagasaki University and was supported by a Kakenhi grant 22-00805. The sediment trap data from Effingham Inlet was obtained through a Natural Sciences and Engineering Research Council of Canada Strategic Project grant to R.T.P. This research was partly supported by the Natural Sciences and Engineering Research Council of Canada (NSERC) through a grant to V.P. Mr Hiromi Saitoh and Kimihiko Maekawa are thanked for assistance during sampling of Saroma Lake. Anna Godhe is thanked for providing a sample from Kattegat for molecular analysis. Two anonymous reviewers and the Editor are acknowledged, whose comments significantly improved the manuscript.

References

- Bolch CJS. 1997. The use of polytungstate for the separation and concentration of living dinoflagellate cysts from marine sediments. *Phycologia* **37**: 472–478.
- Chang AS, Patterson RT, McNeely R. 2003. Seasonal sediment and diatom record from Late Holocene laminated sediments, Effingham Inlet, British Columbia Canada. *Palaios* **18**: 477–494.
- Cho H-J, Matsuoka K. 2001. Distribution of dinoflagellate cysts in surface sediments from the Yellow Sea and East China Sea. *Marine Micropaleontology* **42**: 103–123.
- Coachman LK, Aagaard K. 1974. Physical oceanography of Arctic and Subarctic seas. In *Marine Geology and Oceanography of the Arctic Seas*, Herman Y (ed.). New York: Springer: 1–72.
- Conkright ME, Locarnini RA, Garcia HE, et al. 2002. *World Ocean Atlas 2001: Objective Analyses, Data Statistics, and Figures, CD-ROM Documentation*. National Oceanographic Data Center: Silver Spring, MD, USA.
- Dale B. 1996. Dinoflagellate cyst ecology: modelling and geological applications. In *Palynology: Principles and Applications*, Jansonius J, McGregor DC (eds.). AASP Foundation: Dallas, TX: 1249–1275.
- De Schepper S, Head MJ, Groeneveld J. 2009. North Atlantic Current variability through marine isotope stage M2 (circa 3.3 Ma) during the mid-Pliocene. *Paleoceanography* **24**: PA4206. DOI: 10.1029/2008PA001725.
- de Vernal A, Goyette C, Rodrigues CG. 1989. Contribution palynostratigraphique (dinokystes, pollen et spores) à la connaissance de la Mer Champlain: coupe de Saint-Césaire, Québec. *Canadian Journal for Earth Sciences* **26**: 2450–2464.
- de Vernal A, Henry M, Matthiessen J, et al. 2001. Dinoflagellate cyst assemblages as tracers of sea-surface conditions in the northern North Atlantic, Arctic and sub-Arctic seas: the new ‘n = 677’ database and application for quantitative paleoceanographical reconstruction. *Journal of Quaternary Science* **16**: 681–699.
- Fujii R, Matsuoka K. 2005. Seasonal change of dinoflagellates cyst flux collected in a sediment trap in Omura Bay, West Japan. *Journal of Plankton Research* **28**: 131–147.
- Genovesi B, Shin-Grzebyk M-S, Grzebyk D, et al. 2011. Assessment of cryptic species diversity within blooms and cyst bank of the *Alexandrium tamarense* complex (Dinophyceae) in a Mediterranean lagoon facilitated by semi-multiplex PCR. *Journal of Plankton Research* **33**: 405–414.

- Hallett RI. 1999. *Consequences of environmental change on the growth and morphology of Lingulodinium polyedrum (Dinophyceae) in culture. PhD thesis. University of Westminster.*
- Hay WW. 2008. Evolving ideas about the Cretaceous climate and ocean circulation. *Cretaceous Research* **29**: 725–735.
- Hickey BM. 1998. Coastal oceanography of western North America from the tip of Baja California to Vancouver Island; coastal segment. *Sea* **11**: 345–393.
- Koike K, Horie Y, Suzuki T, et al. 2006. *Protoceratium reticulatum* in northern Japan: environmental factors associated with seasonal occurrence and related contamination of yessotoxin in scallops. *Journal of Plankton Research* **28**: 103–112.
- Krepakevich A, Pospelova V. 2010. Tracing the influence of sewage discharge on coastal bays of Southern Vancouver Island (BC, Canada) using sedimentary records of phytoplankton. *Continental Shelf Research* **30**: 1924–1940.
- Kumar A, Patterson RT. 2002. Dinoflagellate cyst assemblages from Effingham Inlet, Vancouver Island, British Columbia Canada. *Palaeogeography, Palaeoclimatology, Palaeoecology* **180**: 187–206.
- Kusakabe M, Andreev A, Lobanov V, et al. 2002. Effects of the anticyclonic eddies on water masses, chemical parameters and chlorophyll distributions in the Oyashio Current Region. *Journal of Oceanography* **58**: 691–701.
- Limoges A, Kieft J-F, Radi T, et al. 2010. Dinoflagellate cyst distribution in surface sediments along the south-western Mexican coast (14.76° N to 24.75°N). *Marine Micropaleontology* **76**: 104–123.
- Matsuoka K. 1981. Dinoflagellate cysts and pollen in pelagic sediments of the northern part of the Philippine Sea. *Bulletin of the Faculty of Liberal Arts, Nagasaki University (Natural Science)* **21**: 59–70.
- Matsuoka K, Fukuyo Y, Anderson DM. 1989. Methods for modern dinoflagellate cyst studies. In *Red Tides: Biology, Environmental Science and Toxicology*, Okaichi T, Anderson DM, Nemoto T (eds.); Elsevier Science Publishing Co. Inc.: New York; 461–479.
- Matsuoka K, Joyce LB, Kotani Y, et al. 2003. Modern dinoflagellate cysts in hypertrophic coastal waters of Tokyo Bay, Japan. *Journal of Plankton Research* **25**: 1461–1470.
- Mertens KN, Ribeiro S, Bouimetarhan I, et al. 2009. Process length variation in cysts of a dinoflagellate, *Lingulodinium machaerophorum*, in surface sediments investigating its potential as salinity proxy. *Marine Micropaleontology* **70**: 54–69.
- Mertens KN, Dale B, Ellegaard M, et al. 2010. Process length variation in cysts of the dinoflagellate *Protoceratium reticulatum* from surface sediments of the Baltic-Kattegat-Skagerrak estuarine system: a regional salinity proxy. *Boreas* **40**: 242–255.
- Mix AC, Bard E, Eglinton G, et al. 2000. Alkenones and multiproxy strategies in paleoceanographic studies. *Geochemistry Geophysics Geosystems* **1**: 2000GC000056.
- Montresor M, Sgroso S, Proccacci G, et al. 2003. Intraspecific diversity in *Scrippsiella trochoidea* (Dinophyceae): evidence for cryptic species. *Phycologia* **42**: 56–5670.
- Patterson RT, Prokoph A, Kumar A, et al. 2005. Late Holocene variability in pelagic fish scales and dinoflagellate cysts along the west coast of Vancouver Island, NE Pacific Ocean. *Marine Micropaleontology* **55**: 183–204.
- Pospelova V, Kim S-J. 2010. Dinoflagellate cysts in recent estuarine sediment from aquaculture sites of southern South Korea. *Marine Micropaleontology* **76**: 37–51.
- Pospelova V, Chmura GL, Walker HA. 2004. Environmental factors influencing spatial distribution of dinoflagellate cyst assemblages in shallow lagoons of southern New England (USA). *Review of Paleobotany and Palynology* **128**: 7–34.
- Pospelova V, de Vernal A, Pedersen TF. 2008. Distribution of dinoflagellate cysts in surface sediments from the northeastern Pacific Ocean (43–25°N) in relation to sea-surface temperature, salinity, productivity and coastal upwelling. *Marine Micropaleontology* **68**: 21–48.
- Pospelova V, Esenkulova S, Johannessen SC, et al. 2010. Organic-walled dinoflagellate cyst production, composition and flux from 1996 to 1998 in the central Strait of Georgia (BC, Canada): A sediment trap study. *Marine Micropaleontology* **75**: 17–37.
- Prahl FG, Herbert T, Brassell SC, et al. 2000. Status of alkenone paleothermometer calibration: report from Working Group 3. *Geochemistry, Geophysics and Geosystems* **1**: 1–13.
- Price AM, Pospelova V. 2011. High-resolution sediment trap study of organic-walled dinoflagellate cyst production and biogenic silica flux in Saanich Inlet (BC, Canada). *Marine Micropaleontology* **80**: 18–43.
- Radi T, de Vernal A, Peyron O. 2001. Relationships between dinoflagellate cyst assemblages in surface sediment and hydrographic conditions in the Bering and Chukchi seas. *Journal of Quaternary Science* **16**: 667–680.
- Radi T, Pospelova V, de Vernal A, et al. 2007. Dinoflagellate cysts as indicators of water quality and productivity in British Columbia estuarine environments. *Marine Micropaleontology* **62**: 269–297.
- Rahmstorf S. 2002. Ocean circulation and climate during the past 120,000 years. *Nature* **419**: 207–214.
- Richerol T, Rochon A, Blasco S, et al. 2008. Distribution of dinoflagellate cysts in surface sediments of the Mackenzie Shelf and Amundsen Gulf, Beaufort Sea (Canada). *Journal of Marine Systems* **74**: 825–839.
- Rohling EJ. 2000. Paleosalinity: Confidence limits and future applications. *Marine Geology* **163**: 1–11.
- Schlitzer R. 2010. *Ocean Data View*, <http://odv.awi.de> [accessed 1 March 2010].
- Schmidt MW, Spero HJ. 2011. Meridional shifts in the marine ITCZ and the tropical hydrological cycle over the last three glacial cycles. *Paleoceanography* **26**: DOI: 10.1029/2010PA001976.
- Stabeno PJ, Schumacher JD, Ohtani K. 1999. The physical oceanography of the Bering Sea. In *Dynamics of the Bering Sea: A Summary of Physical, Chemical, and Biological Characteristics, and a Synopsis of Research on the Bering Sea*, Loughlin TR, Ohtani K (eds.). Fairbanks (Univ. Alaska Sea Grant): AK; 1–28.
- Takano Y, Horiguchi T. 2005. Acquiring scanning electron microscopical, light microscopical and multiple gene sequence data from a single dinoflagellate cell. *Journal of Phycology* **42**: 251–256.
- Teramoto T. 1987. Kuroshio. In *Encyclopedia of Oceanography*, Wadachi K (ed.). Tokyodoshuppan: Tokyo; 182–192.
- van der Meer MTJ, Sangiorgi F, Baas M, et al. 2008. Molecular isotopic and dinoflagellate evidence for Late Holocene freshening of the Black Sea. *Earth and Planetary Science Letters* **267**: 426–434.
- Vilks G, Wagner FJE, Pelletier BR. 1979. The Holocene marine environment of the Beaufort Shelf. *Geological Survey of Canada Bulletin* **303**: 1–43.
- Wall D, Dale B, Harada K. 1973. Descriptions of new fossil dinoflagellates from the late Quaternary of the Black Sea. *Micropaleontology* **19**: 18–31.
- Wall D, Dale B, Lohman GP, et al. 1977. The environmental and climate distribution of dinoflagellate cysts in modern marine environments from regions in the North and South Atlantic Ocean and adjacent seas. *Marine Micropaleontology* **2**: 121–200.